Supporting information

Interlinking primary grains with lithium boron oxide to enhance stability of $LiNi_{0.8}Co_{0.15}Al_{0.05}O_2$

Fanghui Du [a], Pengpeng Sun [a], Qun Zhou [a], Dong Zeng [b], Die Hu [a], Zhongxu Fan [a], Qi Hao [a], Chengxiang Mei [a], Tao Xu [a], Junwei Zheng [a]**

[a] College of Chemistry, Chemical Engineering and Materials Science & Collaborative Innovation Center of Suzhou Nano Science and Technology, Soochow University, Suzhou 215123, China.

* E-mail: Q. Zhou (zhq@suda.edu.cn); J. Zheng (jwzheng@suda.edu.cn).

[b] Murata Energy Device Wuxi Co., Ltd, Wuxi 214028, China.

To whom all correspondence should be addressed: Q. Zhou, J. Zheng.

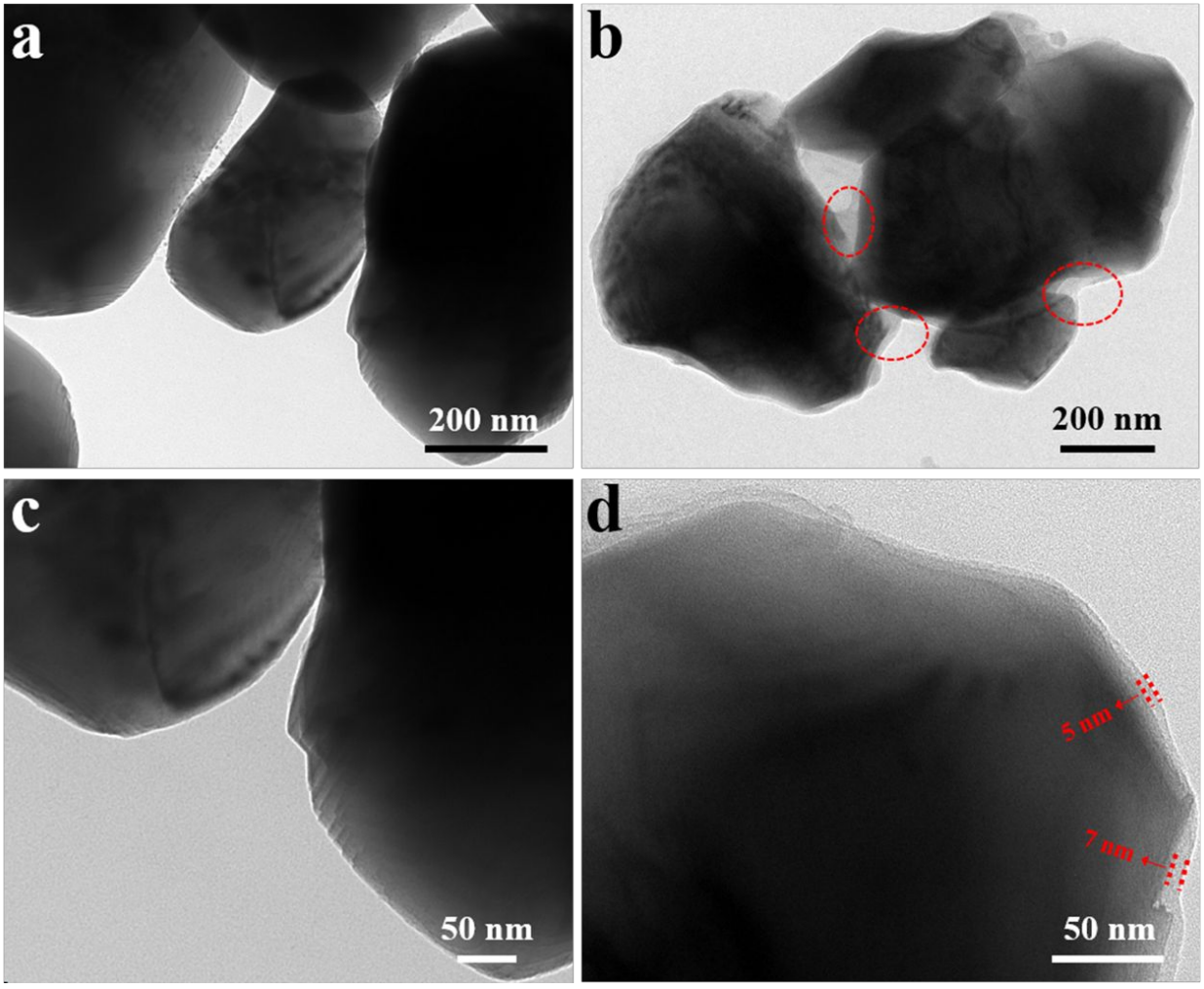

Figure S1. (a) TEM image and (c) magnified TEM image of NCA, (b) TEM image and (d) magnified TEM image of NCA-LB1.

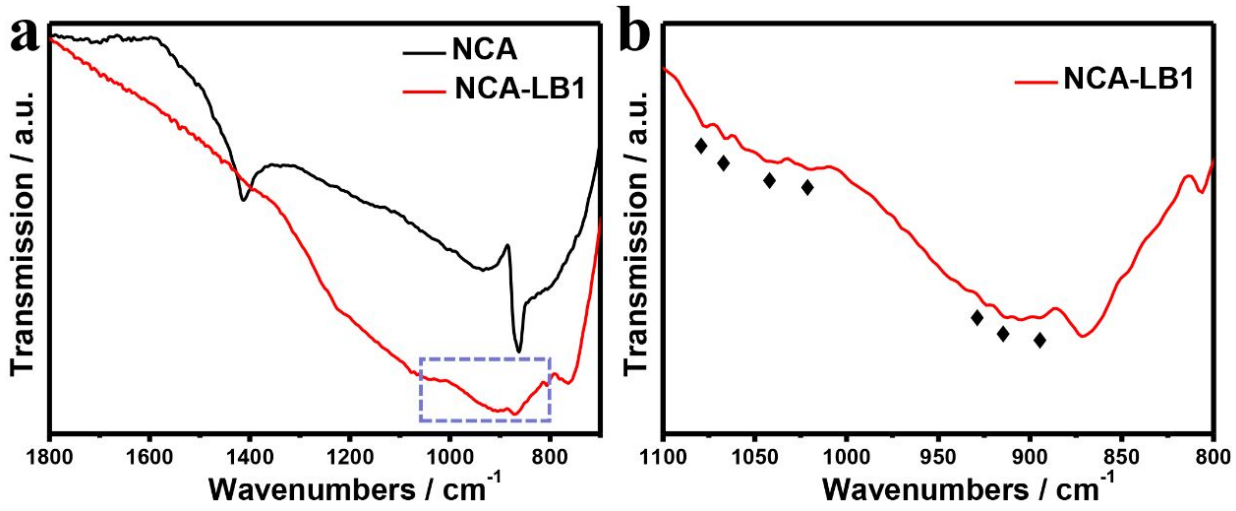

Figure S2. (a) FTIR spectra of NCA and NCA-LB1, (b) Magnified FTIR spectra of NCA-LB1.

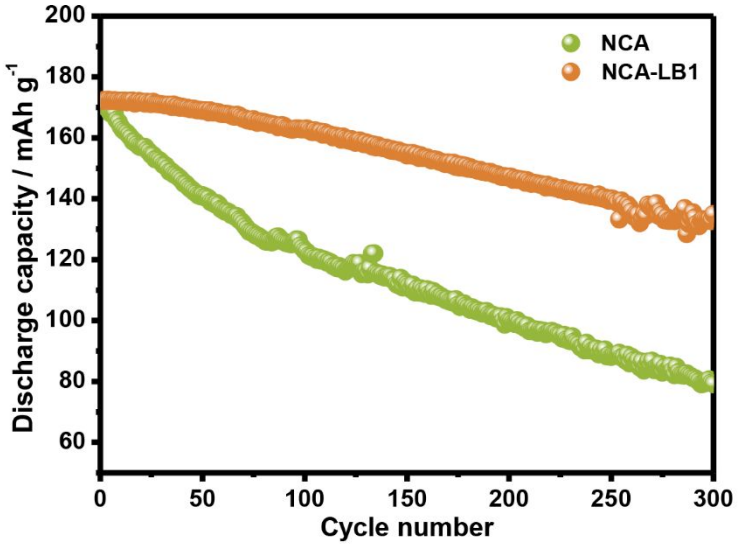

Figure S3. Cycling performance of NCA and NCA-LB1 at 2 C in the voltage range between 2.8 and 4.3 V.

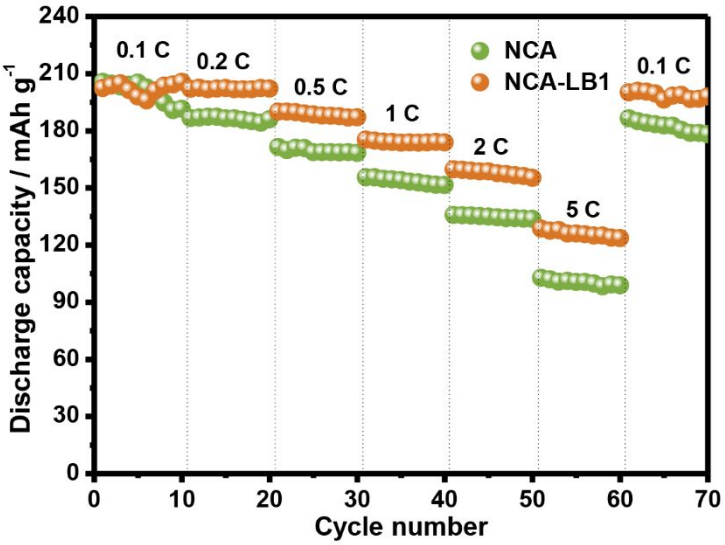

Figure S4. Rate performance of NCA and NCA-LB1 in the voltage range between 2.8 and 4.3 V.

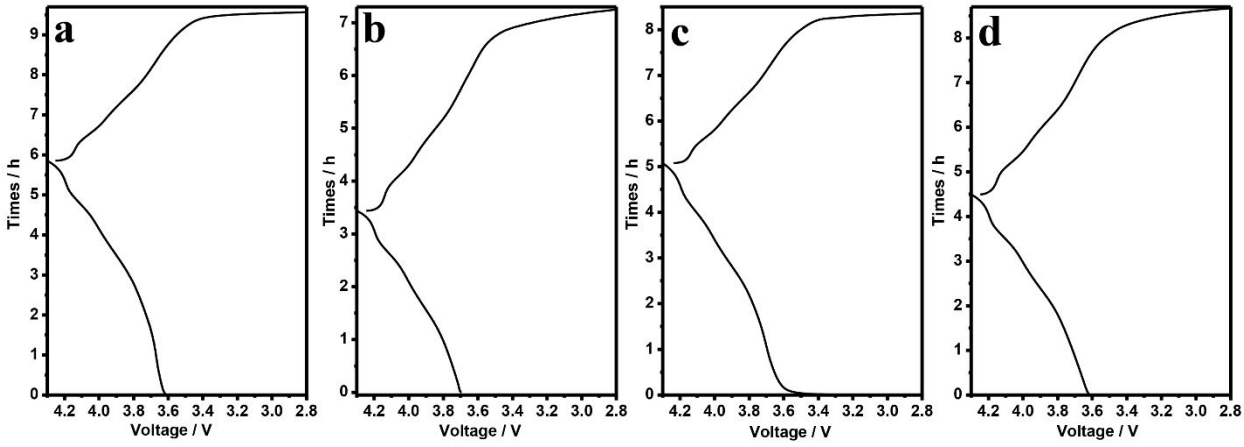

Figure S5. The charge and discharge profiles correspond to *in-situ* XRD: (a) 1st and (b) 50th for NCA, (c) 1st and (d) 50th for NCA-LB1 at 0.2 C (40 mA g^{-1}).

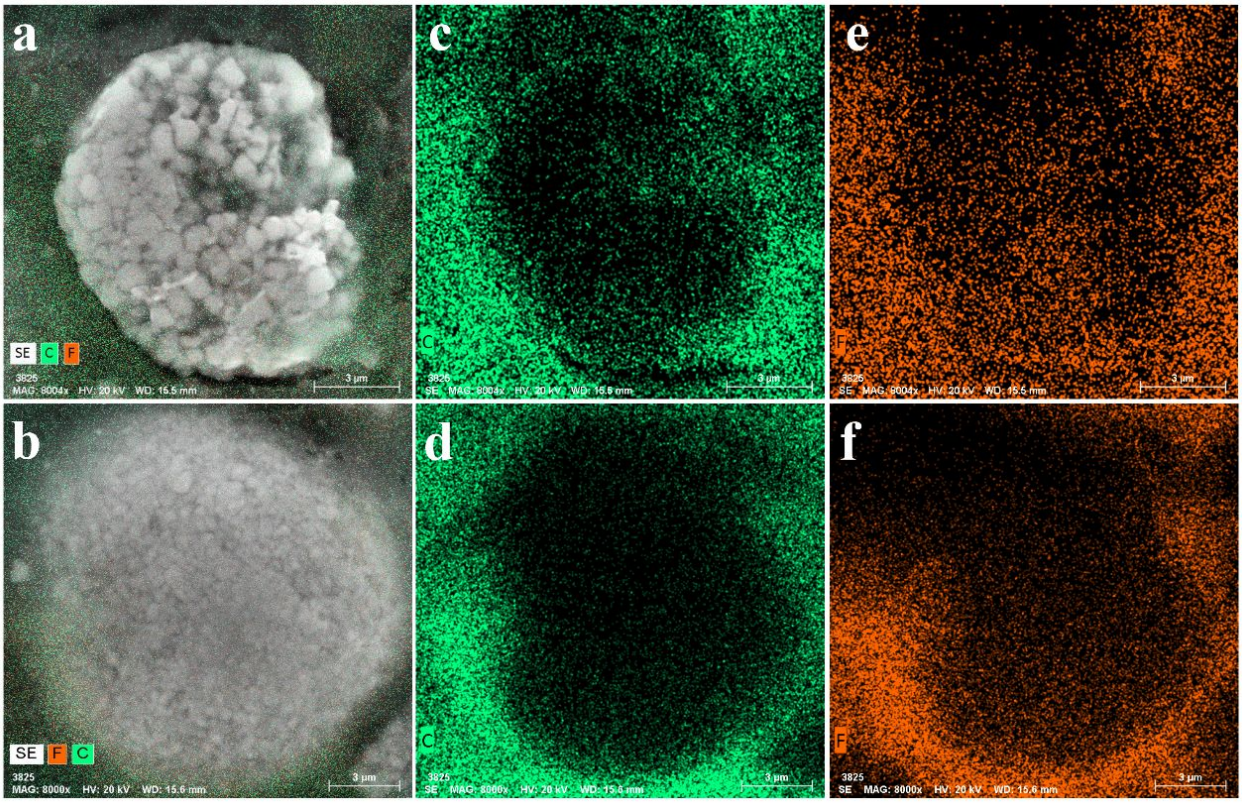

Figure S6. EDX elemental mapping of cycled electrode cross-sections for (a) NCA and (b) NCA-LB1. EDX elemental mapping of C for (c) NCA and (d) NCA-LB1. EDX elemental mapping of F for (e) NCA and (f) NCA-LB1.

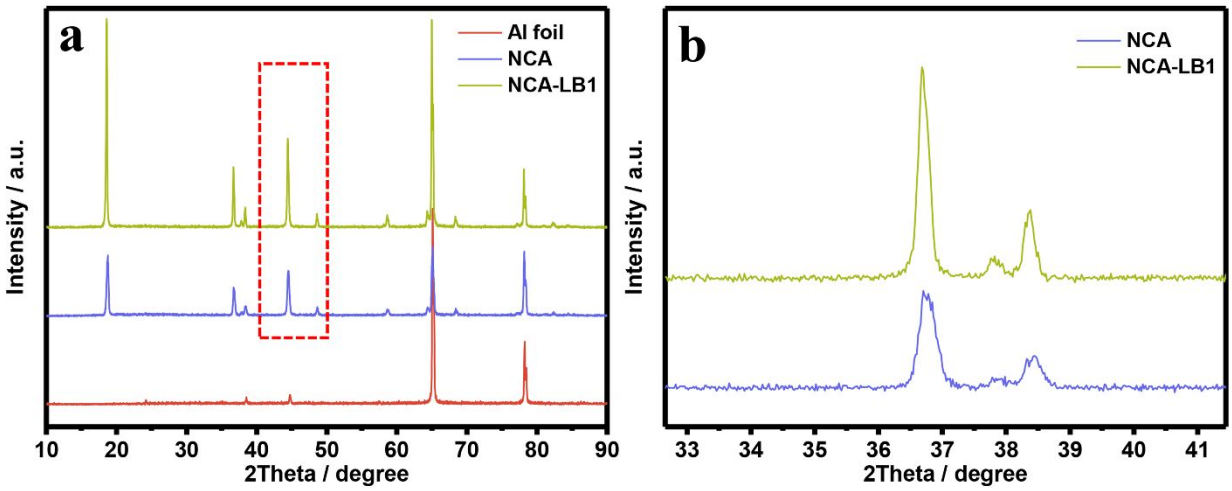

Figure S7. (a) XRD patterns of the cycled of NCA and NCA-LB1 electrodes after 100 cycles, (b) Magnified XRD patterns of the cycled of NCA and NCA-LB1 electrodes.

Table S1 The content of surface residuals of the pristine NCA and NCA-LB1

Samples	Pristine NCA	NCA-LB1
Li_2CO_3	0.498 wt%	0.245 wt%
LiOH	0.137 wt%	0.07 wt%

Table S2 The result of ICP-AES for NCA-LB1.

Concentration of B	430 μg L^{-1}
Mass of dissolved NCA-LB1 powder	20 mg
Volume of solution	50 mL
Mass of Deduced $LiBO_2$	0.0989 mg

Table S3 Electrochemical performance comparison between our sample and other Ni-rich cathodes reported in the literature

Materials	Measurement conditions			Electrochemical		Ref.
	Voltage range (V)	T (K)	Current Density	Cycle number	Retention Rate	
LBO modified $LiNi_{0.8}Co_{0.1}Mn_{0.1}O_2$	2.8-4.3	298	200 mA g^{-1} (1 C)	200	83.0%	1
	2.8-4.3	323	1 C	200	77.3%	
Vanadium compounds modified $LiNi_{0.815}Co_{0.15}Al_{0.035}O_2$	2.75-4.3	298	1 C	100	88.2%	2
PANI-PEG polymers modified $LiNi_{0.8}Co_{0.1}Mn_{0.1}O_2$	2.8-4.3	298	1 C	100	92.4%	3
	2.8-4.3	328	1 C	100	81.4%	
$Na_2S_2O_8$ modified $LiNi_{0.815}Co_{0.15}Al_{0.035}O_2$	2.75-4.3	298	180 mA g^{-1} (1 C)	100	89.2%	4
$LaAlO_3$ modified $LiNi_{0.8}Co_{0.1}Mn_{0.1}O_2$	2.7-4.3	298	170 mA g^{-1} (1 C)	200	84.5%	5
Li_4SiO_4 modified $LiNi_{0.8}Co_{0.15}Al_{0.05}O_2$	2.7-4.3	298	180 mA g^{-1} (1 C)	100	88.08%	6
PANI-PVP modified $LiNi_{0.8}Co_{0.1}Mn_{0.1}O_2$	2.8-4.3	298	1 C	100	88.7%	7
Lithium boron oxide modified $LiNi_{0.8}Co_{0.15}Al_{0.05}O_2$	2.8-4.3	298	2 C	100	93.59%	This work
	2.8-4.3	328	1 C	100	90.87%	

References

(1) Mo, W.; Wang, Z.; Wang, J.; Li, X.; Guo, H.; Peng, W.; Yan, G. Tuning the Surface of $LiNi_{0.8}Co_{0.1}Mn_{0.1}O_2$ Primary Particle with Lithium Boron Oxide toward Stable Cycling. *Chem.*

Eng. J. **2020**, *400*, 125820. https://doi.org/10.1016/j.cej.2020.125820.

(2) Yu, H.; Li, Y.; Hu, Y.; Jiang, H.; Li, C. 110th Anniversary: Concurrently Coating and Doping High-Valence Vanadium in Nickel-Rich Lithiated Oxides for High-Rate and Stable Lithium-Ion Batteries. *Ind. Eng. Chem. Res.* **2019**, *58* (10), 4108–4115. https://doi.org/10.1021/acs.iecr.8b06162.

(3) Cao, Y.; Qi, X.; Hu, K.; Wang, Y.; Gan, Z.; Li, Y.; Hu, G.; Peng, Z.; Du, K. Conductive Polymers Encapsulation to Enhance Electrochemical Performance of Ni-Rich Cathode Materials for Li-Ion Batteries. *ACS Appl. Mater. Interfaces* **2018**, *10* (21), 18270–18280. https://doi.org/10.1021/acsami.8b02396.

(4) Tang, Z.; Bao, J.; Du, Q.; Shao, Y.; Gao, M.; Zou, B.; Chen, C. Surface Surgery of the Nickel-Rich Cathode Material $LiNi_{0.815}Co_{0.15}Al_{0.035}O_2$: Toward a Complete and Ordered Surface Layered Structure and Better Electrochemical Properties. *ACS Appl. Mater. Interfaces* **2016**, *8* (50), 34879–34887. https://doi.org/10.1021/acsami.6b11431.

(5) Li, Y. C.; Zhao, W. M.; Xiang, W.; Wu, Z. G.; Yang, Z. G.; Xu, C. L.; Xu, Y. Di; Wang, E. H.; Wu, C. J.; Guo, X. D. Promoting the Electrochemical Performance of $LiNi_{0.8}Co_{0.1}Mn_{0.1}O_2$ Cathode via $LaAlO_3$ Coating. *J. Alloys Compd.* **2018**, *766*, 546–555. https://doi.org/10.1016/j.jallcom.2018.06.364.

(6) Zheng, J. chao; Yang, Z.; He, Z. jiang; Tong, H.; Yu, W. jing; Zhang, J. feng. In Situ Formed $LiNi_{0.8}Co_{0.15}Al_{0.05}O_2$@$Li_4SiO_4$ Composite Cathode Material with High Rate Capability and Long Cycling Stability for Lithium-Ion Batteries. *Nano Energy* **2018**, *53* (September), 613–621.

https://doi.org/10.1016/j.nanoen.2018.09.014.

(7) Gan, Q.; Qin, N.; Zhu, Y.; Huang, Z.; Zhang, F.; Gu, S.; Xie, J.; Zhang, K.; Lu, L.; Lu, Z. Polyvinylpyrrolidone-Induced Uniform Surface-Conductive Polymer Coating Endows Ni-Rich $LiNi_{0.8}Co_{0.1}Mn_{0.1}O_2$ with Enhanced Cyclability for Lithium-Ion Batteries. *ACS Appl. Mater. Interfaces* **2019**, *11* (13), 12594–12604. https://doi.org/10.1021/acsami.9b04050.